Domain engineering of the transverse piezoelectric coefficient in perovskite ferroelectrics

Matthew Davis, Dragan Damjanovic, Didier Hayem, and Nava Setter

Citation: Journal of Applied Physics **98**, 014102 (2005); doi: 10.1063/1.1929091
View online: https://doi.org/10.1063/1.1929091
View Table of Contents: http://aip.scitation.org/toc/jap/98/1
Published by the American Institute of Physics

Domain engineering of the transverse piezoelectric coefficient in perovskite ferroelectrics

Matthew Davis,[a] Dragan Damjanovic, Didier Hayem, and Nava Setter
Ceramics Laboratory, Ecole Polytechnique Fédérale de Lausanne (EPFL), Lausanne 1015, Switzerland

(Received 24 January 2005; accepted 11 April 2005; published online 6 July 2005)

The transverse piezoelectric coefficient $d_{31}^{\star}$ has been calculated for the six domain-engineered structures occurring in perovskite single crystals, using data for rhombohedral PMN-33PT $[0.67Pb(Mg_{1/3}Nb_{2/3})O_3\text{-}0.33PbTiO_3]$, orthorhombic potassium niobate ($KNbO_3$), tetragonal barium titanate ($BaTiO_3$), and tetragonal lead titanate ($PbTiO_3$). Unlike the longitudinal coefficient ($d_{33}^{\star}$), $d_{31}^{\star}$ is found to be strongly dependent on the transverse (x_1') direction of the as-cut crystal. In general, different domains in a domain-engineered structure will contribute different values of $d_{31}^{\star}$ to that measured. Predicting the global $d_{31}^{\star}$ is therefore difficult since it will depend on the proportion of each domain variant in the structure. Important qualitative differences between tetragonal $BaTiO_3$ and $PbTiO_3$ are discussed. Whereas polarization rotation is important in $BaTiO_3$, $PbTiO_3$ shows a stronger collinear piezoelectric effect due the absence of a low-temperature ferroelectric-ferroelectric phase transition. This leads to low values of $d_{33}^{\star}$ and even positive values of $d_{31}^{\star}$ in the $[111]_C$-poled (C: pseudocubic) domain-engineered structure. The methodology described can be usefully applied to all perovskites. © *2005 American Institute of Physics*. [DOI: 10.1063/1.1929091]

I. INTRODUCTION

Relaxor-ferroelectric single crystals $(1-x)Pb(Mg_{1/3}Nb_{2/3})O_3-xPbTiO_3$ (PMN–xPT) and $(1-x)Pb(Zn_{1/3}Nb_{2/3})O_3-xPbTiO_3$ (PZN–xPT) continue to draw a lot of attention. Following the rediscovery of their very high piezoelectric coefficients for rhombohedral or orthorhombic compositions oriented along the nonpolar $[001]_C$ (C: pseudocubic) direction,[1] much work has concentrated on the concept of domain engineering[2] not only in these materials[3–7] but in simpler perovskite crystals as well.[8–10]

A good definition of "domain engineering" is that given by Bell:[2] A domain-engineered crystal is one which has been poled by the application of a sufficiently high field along one of the possible polar axes of the crystal other than the zero-field polar axis, creating a set of domains in which the polarizations are oriented such that their angles to the poling direction are minimized. In a perovskite material there are therefore three possible sets of poling directions $\langle 111\rangle_C$, $\langle 101\rangle_C$, and $\langle 001\rangle_C$ (if monoclinic phases are ignored). These directions correspond, respectively, to the polar axes of rhombohedral (R, point group $3m$), orthorhombic (O,$mm2$) and tetragonal (T,$4mm$) crystal phases. According to the definition, this results in six possible domain-engineered structures, formed by cutting and poling a perovskite crystal along certain directions; these are listed in Table I. Also given are the three possible monodomain structures $1R$, $1C$, and $1T$ formed by poling a perovskite crystal along its polar axis.

Room-temperature, longitudinal piezoelectric coefficients of up to 2820 pC/N have been measured for $\langle 001\rangle_C$-poled $4R$ domain-engineered PMN-33PT $[0.67Pb(Mg_{1/3}Nb_{2/3})O_3\text{-}0.33PbTiO_3]$.[5] This is nearly 15 times larger than the value ($d_{33}=190$ pC/N) measured for single-domain, rhombohedral PMN–33PT along its polar $\langle 111\rangle_C$ axis.[11,12] The obvious benefits of domain engineering have since been demonstrated for simpler, more classical perovskites as well. A longitudinal piezoelectric coefficient of 203 pC/N was reported by Wada *et al.* for $3T$ $\langle 111\rangle_C$-poled tetragonal barium titanate ($BaTiO_3$).[8] This is more than twice the single-domain value ($d_{33}=90$ pC/N) measured along the $\langle 001\rangle_C$ polar axis.[13]

Many authors have tried to ascertain the origins of the elevated piezoelectric coefficients in domain-engineered crystals. Since domain walls in a domain-engineered structure will not be expected to move under application of an electric field along the poling direction,[1] most work has concentrated on intrinsic, lattice effects. One important intrinsic

TABLE I. Engineered and monodomain states in perovskite single crystals (C denotes reference to the pseudocubic unit cell).

Crystal class	Polar direction (x_3)	Poling direction (x_3')	Polar directions (x_3) for the resultant set of equivalent domainvariants	Domain-engineered structure
Rhombohedral	$\langle 111\rangle_C$	$[111]_C$	$[111]_C$	$1R$
$3m$		$[101]_C$	$[1\text{-}11]_C$, $[111]_C$	$2R$
		$[001]_C$	$[111]_C$, $[11\text{-}1]_C$, $[1\text{-}11]_C$, $[1\text{-}1\text{-}1]_C$	$4R$
Orthorhombic	$\langle 101\rangle_C$	$[111]_C$	$[101]_C$, $[011]_C$, $[110]_C$	$3O$
$mm2$		$[101]_C$	$[101]_C$	$1O$
		$[001]_C$	$[101]_C$, $[011]_C$, $[\text{-}101]_C$, $[0\text{-}11]_C$	$4O$
Tetragonal	$\langle 001\rangle_C$	$[111]_C$	$[001]_C$, $[010]_C$, $[100]_C$	$3T$
$4mm$		$[101]_C$	$[001]_C$, $[100]_C$	$2T$
		$[001]_C$	$[001]_C$	$1T$

[a]Electronic mail: matthew.davis@epfl.ch

characteristic of pervoskite materials is the strong anisotropy of their piezoelectric tensor d_{ijk} in the vicinity of a ferroelectric phase transition, whether induced by electric field, stress, or changes in temperature and composition.[14] Near a phase transition, the direction of maximum measured longitudinal coefficient $d_{33}^{\star}$ is expected to lie at some angle away from the polar axis (" *" is used here to denote coefficients with respect to a noncrystallographic coordinate system—see Sec. II). Using monodomain values for rhombohedral PMN–33PT, $d_{33}^{\star}$ has been calculated along the $[001]_C$ direction as 2309 pC/N.[12,15–17] Upon comparison with the experimental value for the $4R$, $[001]_C$-poled, domain-engineered state of 2820 pC/N it seems that any extrinsic contribution to the response is limited to less than 20%.[16]

As an aside, it has recently been shown that the transverse piezoelectric coefficient ($d_{31}^{\star}$) in $[111]_C$-poled $3T$ $BaTiO_3$ and $[001]_C$-poled $4O$ potassium niobate ($KNbO_3$) does actually increase with an increase of domain-wall density; this suggests that the presence of domain walls in the domain-engineered structure can also play a significant role in the piezoelectric response, especially when the domain structure becomes fine.[9,18] However, these domain-wall-related effects will not be discussed here. Since intrinsic effects will be dominant in most cases, calculations of piezoelectric coefficients along nonpolar directions based on single-domain data are still useful in predicting the properties of domain-engineered crystals. They can be useful in selecting domain-engineered structures worthy of further investigation and, indeed, in helping to quantify the extrinsic contribution to the piezoelectric response when the crystal has been grown and characterized.

Various calculations have already been made of the longitudinal and transverse piezoelectric coefficients ($d_{33}^{\star}$ and $d_{31}^{\star}$)[3,7,15,16,19] although only for a limited number of domain-engineered structures. High $d_{31}^{\star}$ values can be exploited in certain niche applications,[20] for example, in "flextensional" transducers working as "bimorphs" and have recently been reported for $[101]_C$-poled PMN–30PT.[20] In this work, $d_{31}^{\star}$ has been calculated for all six domain-engineered structures, using single-domain data for PMN–33PT (R), $KNbO_3$ (O), and $BaTiO_3$ (T). The $3T$ structure formed by $BaTiO_3$ is then compared to that formed by lead titanate ($PbTiO_3$). It is demonstrated that in certain structures, for a fixed poling direction (named x_3'), the $d_{31}^{\star}$ coefficient measured is strongly dependent on which direction is chosen as the transverse direction (x_1'). Care is therefore needed when designing domain-engineered crystals for use in the transverse mode. Secondly, it is shown that, unlike with the longitudinal coefficient, different variants in the domain-engineered crystal can sometimes contribute different values of $d_{31}^{\star}$ to that measured. In these cases, the $d_{31}^{\star}$ of the final crystal can change significantly depending on which domain variants are present and in what quantity. Finally, it is shown that an important qualitative difference exists between tetragonal crystals which exhibit phase transitions into a lower-symmetry ferroelectric phase ($BaTiO_3$) and those which remain tetragonal at all temperatures ($PbTiO_3$).

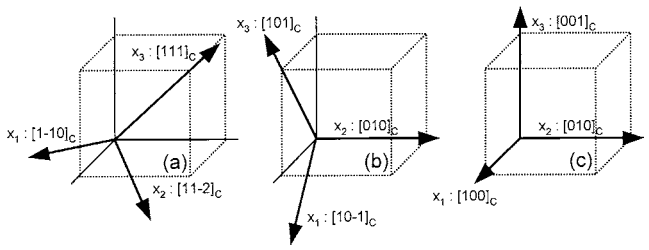

FIG. 1. The sets of axes $\{x_i\}$ used, corresponding to the data given in Table II, for (a) $3m$ rhombohedral, (b) $mm2$ orthorhombic, and (c) $4mm$ tetragonal monodomains.

II. METHODOLOGY

Calculations of piezoelectric coefficients (d_{ijk}) as a function of orientation are done via coordinate transforms.[21] In all cases, they must start with a complete set of coefficients for the single-domain state defined with reference to an orthogonal set of axes $\{x_1,x_2,x_3\}$. In perovskites it is useful to define these axes with respect to those of the cubic parent phase—i.e., the basis set formed by the $\langle 001\rangle_C$ psuedocubic directions. In this paper we use the orthogonal sets of axes for the rhombohedral ($R,3m$), orthorhombic ($O,mm2$), and tetragonal ($T,4mm$) crystal classes as given in Ref. 21 (i.e., as defined relative to one or more symmetry elements of the point group). Defined in this way the piezoelectric tensors d_{ijk} for each crystal class have a certain "standard" form. We also use a standard right-handed set. The x_3 direction is always the crystal's polar axis, or the direction of spontaneous polarization $\mathbf{P}_s$. For a $4mm$ crystal $x_1{:}[100]_C$, $x_2{:}[010]_C$, and $x_3{:}[001]_C$ define the obvious set of axes (":" here means "parallel to"). However, for the rhombohedral and orthorhombic classes there is still some arbitrariness in our choice of axes which can switch or invert the sign of certain coefficients even if the form of the tensor is unchanged.[12] For the rhombohedral $3m$ class, we choose $x_1{:}[1\text{-}10]_C$, $x_2{:}[11\text{-}2]_C$, and $x_3{:}[111]_C$ and exercise caution in using the single-domain data from the literature.[12] For the orthorhombic $mm2$ class, we choose $x_1{:}[10\text{-}1]_C$, $x_2{:}[010]_C$, and $x_3{:}[101]_C$. All three sets of axes are shown with respect to the basis set of the pseudocubic unit cell in Fig. 1.

The materials chosen for study were PMN–33PT, potassium niobate ($KNbO_3$), and barium titanate ($BaTiO_3$) which are rhombohedral $3m$, orthorhombic $mm2$, and tetragonal $4mm$ at room temperature, respectively.[11,13,22] Complete sets of material properties as measured by Zhang *et al.*[11] and Zgonik *et al.*[13,22] are available for all of these materials, at room temperature, corresponding to the axes chosen. Lead titanate ($PbTiO_3$), also $4mm$ tetragonal,[23] was investigated for comparison with $BaTiO_3$. Good $PbTiO_3$ crystals cannot easily be grown, and are difficult to characterize due to their high conductivity. Therefore, the monodomain values used for $PbTiO_3$ were those calculated by Haun *et al.*[24] using phenomenological theory, although it would change little here to use those measured experimentally.[23] All the values of piezoelectric coefficient used (d_{ijk} or d_{ij} in condensed notation), corresponding to the sets of axes given above, are listed in Table II.

As stated above, using these monodomain values we can

TABLE II. Monodomain piezoelectric coefficients used in this study, based on the coordinate systems shown in Fig. 1. The room-temperature data are from Zhang *et al.* (see Ref. 11) (PMN–33PT), Zgonik *et al.* (see Ref. 13 and 22) ($BaTiO_3$ and $KNbO_3$), and Haun *et al.* (see Ref. 24) ($PbTiO_3$). The values in parentheses are not independent.

Material	d_{15}/[pC/N]	d_{22}/[pC/N]	d_{24}/[pC/N]	d_{31}/[pC/N]	d_{32}/[pC/N]	d_{33}/[pC/N]
PMN–33PT	4100	−1340	(4100)	−90	(−90)	190
$BaTiO_3$	564		(564)	−33.4	(−33.4)	90
$PbTiO_3$	56.1		(56.1)	−23.1	(−23.1)	79.1
$KNbO_3$	206		156	9.8	−19.5	29.3

calculate the piezoelectric coefficient d^*_{ijk} that we would measure in some other system of axes via a coordinate transform. Essentially, when we cut a crystal and measure its piezoelectric properties, we choose a measurement coordinate system with axes $\{x'_1, x'_2, x'_3\}$. In a domain-engineered crystal x'_3 is thus the poling direction. To calculate the piezoelectric coefficient we make a coordinate transformation from the crystallographic coordinate system $\{x_1, x_2, x_3\}$, with which we defined d_{ijk}, to this set. This is done using the transformation matrix a_{ij} as written in Eq. (1).

$$d^*_{ijk} = a_{im} a_{jn} a_{ko} d_{mno}, \tag{1}$$

a_{ij} is defined as the cosines of the angles α_{ij} between the "old" axis x_j and the "new" axis x'_i ($a_{ij} = \cos \alpha_{ij}$). Equivalently, a_{ij} can be written in terms of the Euler angles (ϕ, θ, ψ) which describe sequential, anticlockwise rotations of the coordinate system about the x_3 axis (by ϕ), the then-rotated x_1 axis (θ), and the final x'_3 axis (ψ). This is known as the *ZXZ* convention.[25] In terms of the three Euler angles, the elements of a_{ij} are then:

$$\begin{aligned}
a_{11} &= \cos\psi \cos\phi - \cos\theta \sin\phi \sin\psi, \\
a_{12} &= \cos\psi \sin\phi + \cos\theta \cos\phi \sin\psi, \\
a_{13} &= \sin\psi \sin\theta, \\
a_{21} &= -\sin\psi \cos\phi - \cos\theta \sin\phi \cos\psi, \\
a_{22} &= -\sin\psi \sin\phi + \cos\theta \cos\phi \cos\psi, \\
a_{23} &= \cos\psi \sin\theta, \\
a_{31} &= \sin\theta \sin\phi, \\
a_{32} &= -\sin\theta \cos\phi, \\
a_{33} &= \cos\theta.
\end{aligned} \tag{2}$$

Other definitions of the Euler angles are also possible, which will give different forms of a_{ij}.

TABLE III. Low-index choices of measurement direction x'_1 for the three poling directions relevant to domain engineering in perovskites.

Poling direction (x'_3)	Possible choices of measurement direction (x'_1)
$[111]_C$	$\pm[10\text{-}1]_C$, $\pm[11\text{-}2]_C$, $\pm[01\text{-}1]_C$, $\pm[\text{-}12\text{-}1]_C$, $\pm[\text{-}110]_C$, $\pm[\text{-}211]_C$
$[101]_C$	$\pm[10\text{-}1]_C$, $\pm[11\text{-}1]_C$, $\pm[12\text{-}1]_C$, $\pm[010]_C$, $\pm[\text{-}121]_C$, $\pm[\text{-}111]_C$
$[001]_C$	$\pm[100]_C$, $\pm[110]_C$, $\pm[010]_C$, $\pm[\text{-}110]_C$

When we cut a domain-engineered crystal for measurement we must first choose our poling axis x'_3 ($\langle 111\rangle_C$, $\langle 101\rangle_C$, or $\langle 001\rangle_C$), by setting the first two Euler angles ϕ and θ. We then have certain freedoms in how we cut the crystal to define the other two perpendicular measurement directions x'_1 and x'_2 in the "poling plane" (the plane of the crystal perpendicular to the poling direction). In choosing x'_1 (and therefore x'_2) we are setting the third Euler angle ψ, as shown in Fig. 2(a); the three poling planes are shown in Fig. 2(b). Any choice of x'_1 is possible but we shall only consider the most obvious directions: those of type $\langle 112\rangle_C$, $\langle 110\rangle_C$, and $\langle 100\rangle_C$. For example, if we choose $[001]_C$ as the poling direction, we can set x'_1 along either the edges of the pseudocubic unit cell ($\pm[100]_C$ and $\pm[010]_C$) or its face diagonals ($\pm[1\text{-}10]_C$ and $\pm[110]_C$). There are therefore $4 \times 2 = 8$ ways to define x'_1 in the $(001)_C$ plane. For both $[111]_C$ and $[101]_C$ poling directions there are $6 \times 2 = 12$ possible ways of defining x'_1 in the $(111)_C$ and $(101)_C$ planes, respectively. All of these definitions of x'_1 are listed in Table III and shown schematically in Fig. 3, for the three poling directions. The direction x'_2 is not given but is, in all cases, the direction forming an orthogonal, right-handed set with the other two.

Using this methodology, d^*_{33} and d^*_{31} were calculated for all of the domain-engineered structures listed in Table I,

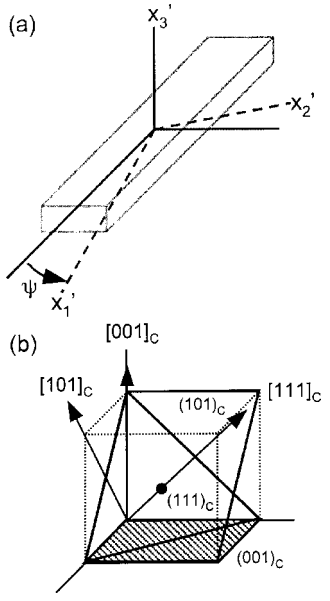

FIG. 2. (a) Definition of the third Euler angle ψ with respect to the measurement axes x'_1, x'_2, and x'_3 shown for a d_{31} resonator. (b) The three "poling planes" $(111)_C$, $(101)_C$, and $(001)_C$ perpendicular to the three poling directions $[111]_C$, $[101]_C$, and $[001]_C$, respectively.

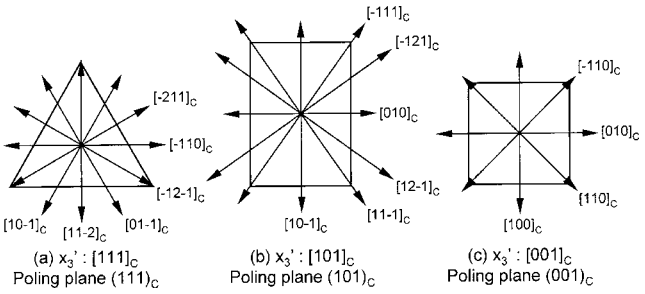

FIG. 3. Possible choices of the measurement direction x_1' for perovskite crystals cut and poled along x_3':$[111]_C$ (a), $[101]_C$ (b), and $[001]_C$ (c). x_3' is perpendicular to the plane of the paper. The directions are shown in the $(111)_C$, $(101)_C$, and $(001)_C$ poling planes, respectively.

based on the monodomain data for PMN–33PT (R), $KNbO_3$ (O), and $BaTiO_3$ (T) in Table II, for all of the x_1' directions listed in Table III. Calculations were also made for the $3T$ structure formed by poling $PbTiO_3$ along the $[111]_C$ direction.

III. RESULTS AND DISCUSSION

It turns out that, for $3m$, $mm2$, and $4mm$ crystal classes, the longitudinal piezoelectric coefficient d_{33}^* is never dependent on the third Euler angle ψ (i.e., that defining x_1') although d_{31}^* always is. x_1' is thus an important direction when we orient our bar-shaped d_{31} resonator in the plane of the crystal [Fig. 2(a)]. However, it does not matter which axes we choose as x_1' and x_2' for our elongated d_{33} resonator; only the axial direction x_3' (defined by Euler angles ϕ and θ) matters.

The angle ψ is particularly important because it can be interpreted in two ways. Firstly, and as stated above, it defines the measurement direction x_1' (after x_3' has been chosen) when calculating the response of a single, fixed variant in the domain-engineered structure. Secondly, it will also define the variant in the domain-engineered structure whose contribution we are considering when the measurement directions x_1' and x_3' are both fixed. This is shown graphically in Fig. 4 taking two variants in the $4R$ structure as an example.

Each variant in a domain-engineered structure will have a different polar axis (x_3) as one of a set of its own, individual crystallographic axes $\{x_i\}$. Critically, for a domain-engineered structure and fixed measurement axes $\{x_i'\}$ the first two Euler angles ϕ and θ will be the same for every variant whereas ψ will not. For a domain-engineered structure nR (or nO or nT), the variants in the structure will be rotated relative to each other by an angle $\Delta\psi=360°/n$ about the poling axis. For a $[001]_C$-poled rhombohedral crystal ($4R$) the four variants are related to each other by rotations of $\Delta\psi=90°$.

It follows that the contribution to d_{33}^* from each variant in a domain-engineered structure, which can depend only on θ and ϕ, will be the same; it only matters that the polar axis (x_3) in each variant is equally inclined to the poling direction. In contrast, since d_{31}^* is a function of ψ, different variants in the domain-engineered structure might therefore give different contributions to the transverse piezoelectric coefficient. This possibility is explored below for the six possible

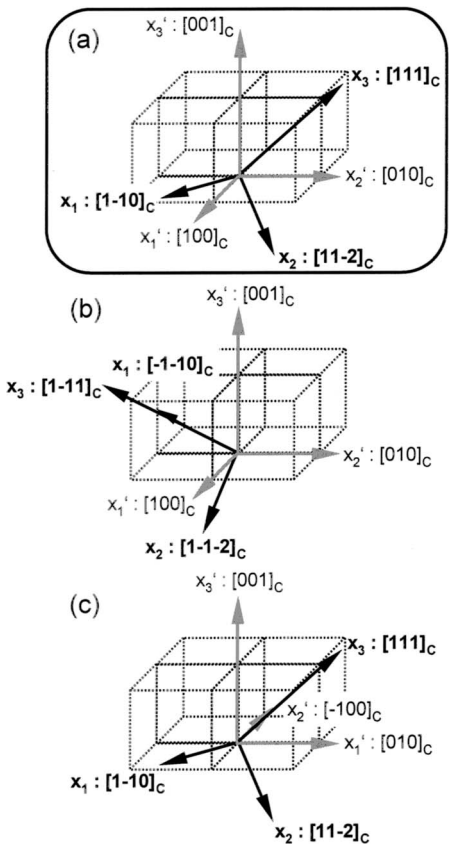

FIG. 4. Meaning of the angle ψ as a rotation about the poling axis x_3'. The inset figure (a) defines the coordinate transform from $\{x_i\}$ to $\{x_i'\}$ relevant to a $4R$ domain-engineered structure for Euler angles $\phi=0°$ and $\theta=54.74°$ (for $\psi=45°$ as shown we have x_1':$[100]_C$). A further rotation of $\Delta\psi=90°$ corresponds to rotating the measurement direction x_1' from $[100]_C$ to $[010]_C$ (c). This is equivalent to starting with another variant (that with polar direction x_3:$[1-11]_C$) and transforming to the coordinate system with x_1':$[100]_C$ (b). Rotating $\{x_i'\}$ *anticlockwise* by $\Delta\psi$ is equivalent to rotating $\{x_i\}$ by $\Delta\psi$ *clockwise*.

domain-engineered structures. Results for d_{33}^* and d_{31}^* are summarized in Tables IV and V, respectively. Also given in the tables are the first two Euler angles used in the calculation as relevant to the poling direction and the choice of basis defined in Fig. 1. For all seven cases investigated the function $d_{31}^*(\psi)$ was found to be of the form $X\cos^2\psi+Y\sin^2\psi$ where X and Y are the upper and lower bounds of the function. In most, but not all, cases X and Y are negative.

A. PMN–33PT

Taking the values shown in Table II for rhombohedral PMN–33PT and transforming to the $[001]_C$ direction (taking $\phi=0°$, $\theta=54.74°$), we find a value of $d_{33}^*=2309$ pC/N (see Table IV), independent of the angle ψ and, therefore, the choice of x_1'. To reiterate, all four variants in the $4R$ structure will give the same contribution to the measured d_{33}^* value. As stated in Sec. I this value, and thus the crystal anisotropy of PMN–33PT at room temperature, will account for as much as 80% of the multidomain value (2820 pC/N).

For PMN–33PT in the $4R$ structure, d_{31}^* *is* found to be, albeit only slightly, dependent on our choice of x_1'. d_{31}^* varies as a function of ψ between $X=-1146.1$ pC/N and $Y=-1157.6$ pC/N, as shown in Fig. 5(a). The function

TABLE IV. Longitudinal piezoelectric coefficients d_{33}^* calculated for possible domain-engineered structures of $BaTiO_3$, $KNbO_3$, $PbTiO_3$, and PMN–33PT at room temperature. The Euler angles (ϕ and θ) relevant to the coordinate transform made are given. Also listed is the monodomain value of d_{33} corresponding to that along the polar axis of the crystal (x_3).

Material	Monodomain value along polar axis, d_{33}/[pC/N]	Poling direction (x_3')	Domain engineered structure	ϕ/[°]	θ/[°]	Value calculated along poling direction, d_{33}^*/[pC/N]
PMN–33PT	190	$[101]_C$	2*R*	60	35.26	937
		$[001]_C$	4*R*	0	54.74	2309
$KNbO_3$	29.3	$[111]_C$	3*O*	0	−35.26	53.1
		$[001]_C$	4*O*	90	−45	86.7
$BaTiO_3$	90	$[111]_C$	3*T*	−45	−54.7	221.5
		$[101]_C$	2*T*	90	45	219.4
$PbTiO_3$	79.1	$[111]_C$	3*T*	−45	−54.7	27.9

$d_{31}^*(\phi=0°, \theta=54.74°, \psi)$ is given explicitly in Table V. The fact that d_{31}^* is not affected by a rotation of $\Delta\psi=180°$ is intuitive since stress and strain have no sense of "polarity." The position $\psi=0°$ corresponds here to $x_1':[1\text{-}10]_C$ where d_{31}^* is least negative. The most negative d_{31}^* value of −1157.6 is found at $\psi=\pm 90°$ corresponding to $x_1':\pm[110]_C$.

Figure 6(a) shows d_{31}^* graphically for the various choices of x_1' in the $(001)_C$ poling plane. The values given here are only valid for the variant in the domain-engineered structure with polar axis $\mathbf{P}_S$ (or x_3):$[111]_C$, as shown projected onto $(001)_C$ as a thick arrow. The diagram can be used to calculate the contribution from the other three domain variants in the structure, when the x_1' direction is fixed. For example with $x_1':[1\text{-}10]_C$, the contribution from the variant shown ($x_3:[111]_C$) is −1146.1 pC/N. Calculating the d_{31}^* contribution from the variant in the structure with $x_3:[1\text{-}11]_C$ involves rotating the projected $[111]_C$ polar vector by 90° clockwise. Therefore, equivalently to this from consideration of Fig. 4, we can simply rotate the x_1' direction in Fig. 6(a) by the same amount anticlockwise and read the value directly from the diagram. The contribution from this domain variant is thus −1157.6 pC/N.

We can similarly see all the permutations: if we choose x_1' as one of the face diagonals of the pseudocubic cell $\langle 110\rangle_C$, two variants will yield a value of d_{31}^* =−1146.1 pC/N and the other two will contribute d_{31}^* =−1157.6 pC/N. However, if we choose x_1' to be along one of the edges of the pseudocubic unit cell, $\langle 100\rangle_C$, each variant will contribute the same value of d_{31}^*=−1151.8 pC/N. Two of the four domain variants in this case correspond to (a) and (b) of Fig. 4. The value here of −1151.8 pC/N accounts for more than 80% of the experimental value (d_{31}^* =−1330 pC/N) reported by Zhang *et al.*[5] Most interestingly, in the former case with x_1' along a face diagonal $\langle 110\rangle_C$, the contributions from the different variants in the domain-

TABLE V. Transverse piezoelectric coefficients d_{31}^* calculated for possible domain-engineered structures of $BaTiO_3$, $KNbO_3$, $PbTiO_3$, and PMN–33PT, at room temperature, as a function of the third Euler angle ψ. Also given is the x_1' measurement direction corresponding to $\psi=0°$.

Material	Poling direction (x_3')	Domain engineered structure	$d_{31}^*(\psi)$/[pC/N]	x_1^* direction for $\psi=0$
PMN-33PT	$[101]_C$	2*R*	$+700.2\cos^2\psi-1628.9\sin^2\psi$	$[10\text{-}1]_C$
	$[001]_C$	4*R*	$-1146.1\cos^2\psi-1157.6\sin^2\psi$	$[1\text{-}10]_C$
$KNbO_3$	$[111]_C$	3*O*	$+8.0\cos^2\psi-45.1\sin^2\psi$	$[10\text{-}1]_C$
	$[001]_C$	4*O*	$-13.8\cos^2\psi-59.0\sin^2\psi$	$[010]_C$
$BaTiO_3$	$[111]_C$	3*T*	$-19.3\cos^2\psi-188.9\sin^2\psi$	$[1\text{-}10]_C$
	$[101]_C$	2*T*	$-23.6\cos^2\psi-179.4\sin^2\psi$	$[010]_C$
$PbTiO_3$	$[111]_C$	3*T*	$-13.3\cos^2\psi+4.4\sin^2\psi$	$[1\text{-}10]_C$

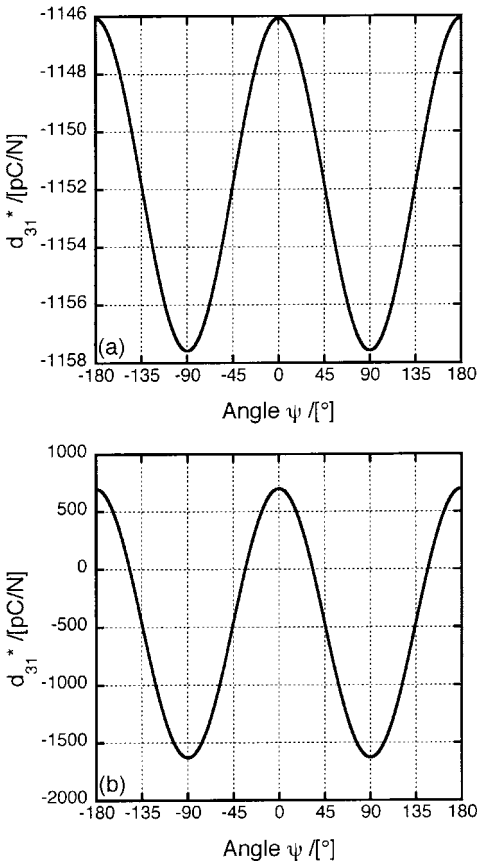

FIG. 5. (a) $d_{31}^*(\phi=0°, \theta=54.74°)$ calculated as a function of ψ in the $(001)_C$ poling plane of 4*R* domain-engineered PMN–33PT. $\psi=0°$ and $\psi=45°$ correspond to $x_1':[1\text{-}10]_C$ and $x_1':[100]_C$, respectively. (b) $d_{31}^*(\phi=60°, \theta=35.26°)$ calculated as a function of ψ in the $(101)_C$ poling plane of 2*R* domain-engineered PMN–33PT. $\psi=0°$ and $\psi=90°$ correspond to $x_1':[10\text{-}1]_C$ and $x_1':[010]_C$, respectively.

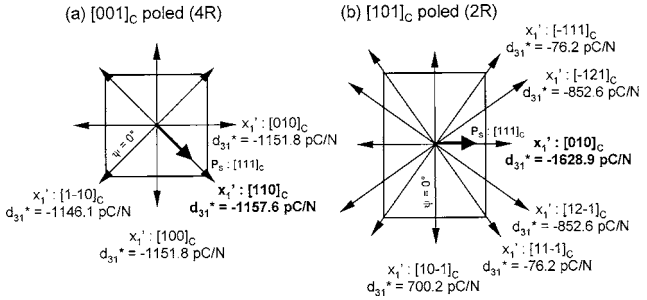

FIG. 6. (a)The $(001)_C$ poling plane of a $4R$ sample of PMN–33PT (with $x_3':[001]_C$). The values of d_{31}^* calculated for various choices of measurement direction x_1' are shown for a domain with spontaneous polarization $\mathbf{P}_S$ (or x_3): $[111]_C$ ($\mathbf{P}_S$ is also shown projected onto the plane as a thick arrow). The most negative value is shown in bold and lies at $x_1':\pm[110]_C$. (b) The $(101)_C$ poling plane of a $2R$ sample of PMN–33PT (with $x_3':[101]_C$). The values of d_{31}^* calculated for various choices of measurement direction x_1' are shown for a domain with spontaneous polarization $\mathbf{P}_S$ (or x_3): $[111]_C$ ($\mathbf{P}_S$ is also shown projected onto the plane as a thick arrow). The most negative value is shown in bold and lies at $x_1':\pm[010]_C$.

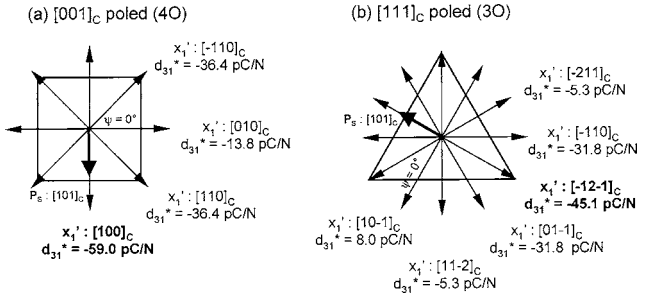

FIG. 7. (a) The $(001)_C$ poling plane of a $4O$ sample of $KNbO_3$ (with $x_3':[001]_C$). The values of d_{31}^* calculated for various choices of measurement direction x_1' are shown for a domain with spontaneous polarization $\mathbf{P}_S$ (or x_3): $[101]_C$ ($\mathbf{P}_S$ is also shown projected onto the plane as a thick arrow). The most negative value is shown in bold and lies at $x_1':\pm[100]_C$. (b) The $(111)_C$ poling plane of a $3O$ sample of $KNbO_3$ (with $x_3':[111]_C$). The values of d_{31}^* calculated for various choices of measurement direction x_1' are shown for a domain with spontaneous polarization $\mathbf{P}_S$ (or x_3):$[101]_C$ ($\mathbf{P}_S$ is also shown projected onto the plane as a thick arrow). The most negative value is shown in bold and lies at $x_1':\pm[-12\text{-}1]_C$.

engineered crystal are *different*. The value of d_{31}^* measured, therefore, will be strongly dependent on the relative presences of each domain, something which will be discussed later.

Lastly, it should be noted that the direction of largest (most negative) d_{31}^* is found where the projection of the variant's polar direction in the $(001)_C$ plane is *parallel* to the measurement axis x_1'. The most positive response is found where these two directions are perpendicular.

The other domain-engineered structure for a rhombohedral crystal, $2R$, is that formed upon poling along $[101]_C$. The first two Euler angles relevant to this transformation are $\phi=60°$ and $\theta=35.26°$, as listed in Table IV. The value of d_{33}^* estimated for this domain-engineered structure is 937 pC/N, still nearly five -times larger than the monodomain value.

The transverse piezoelectric response for $[101]_C$-poled PMN–33PT is more interesting. The function $d_{31}^*(\phi=60°, \theta=35.26°, \psi)$ is shown in Fig. 5(b) where $\psi=0$ corresponds to $x_1':[10\text{-}1]_C$. The values are plotted, for all 12 choices of x_1' in the plane of $(101)_C$, in Fig. 6(b). In this structure, both variants are rotated by $\Delta\psi=180°$ relative to each other so, for any given choice of x_1', both must contribute exactly the same value of d_{31}^*. d_{31}^* varies here between $X=+700.2$ pC/N (for $x_1':\pm[10\text{-}1]_C$) and $Y=-1628.9$ pC/N (for $x_1':\pm[010]_C$).

As for the $4R$ structure, the most negative value of d_{31}^* (-1628.9 pC/N) is found where x_1' is parallel to the projection of the polar axis into the $(101)_C$ plane. This value is more than 19 times larger than the monodomain value of -90 pC/N for PMN–33PT (Table II). And as for the $4R$ structure, the large enhancement is related directly to the very large value of d_{15} (=4100 pC/N) in PMN–33PT. With the same domain-engineered configuration ($2R$) an even higher value of d_{31}^* (-2517 pC/N) was recently reported for rhombohedral PMN–30PT.[20] With the $2R$ structure in PMN$-x$PT, therefore, we can engineer very high d_{31}^* values, by careful choice of x_1', without worrying about the relative presences of each domain. This might be exploitable in certain applications.

B. Potassium niobate ($KNbO_3$)

Using the values for monodomain potassium niobate and transforming to $x_3':[001]_C$ ($\phi=90°, \theta=-45°$) we calculate a value of $d_{33}^*=86.7$ pC/N, independent of ψ. This accounts for the largest part of the equivalent, experimental value (92 pC/N) measured for the $4O$ structure by Nakamura *et al.*[10] The transverse piezoelectric coefficient $d_{31}^*(\phi=90°, \theta=-45°, \psi)$ is a strong function of ψ, varying between $X=-13.8$ pC/N and $Y=-59.0$ pC/N (Table V). $\psi=0°$ corresponds to $x_1':[010]_C$. The values are shown graphically in Fig. 7(a) where d_{31}^* is given for various x_1' for a domain with $\mathbf{P}_S:[101]_C$. Also marked is the projection of this polar axis onto the $(001)_C$ plane, the direction parallel to which x_1' yields the most negative value of d_{31}^* ($x_1':\pm[100]_C$).

In the $4O$ structure all domain variants are related by rotations of $\Delta\psi=45°$. If we choose x_1' along a direction $\langle 110\rangle_C$, all four variants will contribute the same value of d_{31}^* to the overall: we can expect to measure a value of -36.4 pC/N. However, as for the $4R$ structure, if we choose an edge of the pseudocubic unit cell as x_1' (i.e., $\langle 100\rangle_C$) two variants will contribute a value of $d_{31}^*=-13.8$ pC/N and the other two will contribute the more negative value of -59.0 pC/N. The transverse piezoelectric coefficient measured will be some function of these two values depending on the relative proportion of domains, of each variant, in the poled crystal.

The other possible domain-engineered structure for an orthorhombic crystal is $3O$, that formed upon poling along the $[111]_C$ direction. d_{33}^* calculated in this case (for $\phi=0°$, $\theta=-35.26°$) is 53.1 pC/N, nearly twice as much as the monodomain value of 29.3 pC/N (Table IV). d_{31}^* varies between $X=+8.0$ pC/N and $Y=-45.1$ pC/N (Table V) where $\psi=0°$ corresponds to $x_1':[10\text{-}1]_C$. As for the $2R$ structure the upper and lower bounds of d_{31}^* are of different sign.

The results are shown figuratively in Fig. 7(b) in the plane $(111)_C$, perpendicular to the poling direction. The most negative value is found for $x_1':\pm[-12\text{-}1]_C$ parallel to the projection of $\mathbf{P}_S$. In the $3O$ structure we will have three variants rotated relative to each other by $\Delta\psi=120°$. Therefore, de-

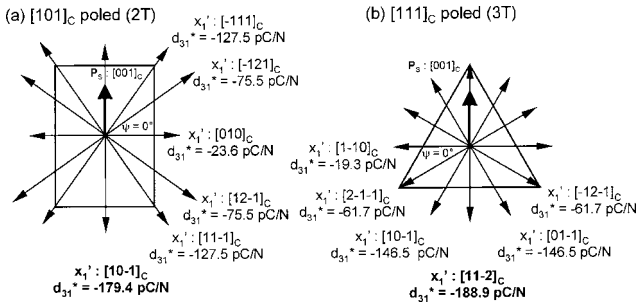

FIG. 8. (a) The $(101)_C$ poling plane of a $2T$ sample of $BaTiO_3$ (with x_3':$[101]_C$). The values of d_{31}^* calculated for various choices of measurement direction x_1' are shown for a domain with spontaneous polarization $\mathbf{P}_S$ (or x_3): $[001]_C$ ($\mathbf{P}_S$ is also shown projected onto the plane as a thick arrow). The most negative value is shown in bold and lies at x_1': $\pm[10\text{-}1]_C$. (b) The $(111)_C$ poling plane of a $3T$ sample of $BaTiO_3$ (with x_3':$[111]_C$). The values of d_{31}^* calculated for various choices of measurement direction x_1' are shown for a domain with spontaneous polarization $\mathbf{P}_S$ (or x_3):$[001]_C$ ($\mathbf{P}_S$ is also shown projected onto the plane as a thick arrow). The most negative value is shown in bold and lies at x_1': $\pm[11\text{-}2]_C$.

pending on our choice of x_1', there will be a set of three different contributions to d_{31}^* from the three variants. For x_1' along one of the directions $\langle 11\text{-}2\rangle_C$ in the $(111)_C$ plane, two domains will contribute a value of −5.3 pC/N and the third will contribute a larger value of −45.1 pC/N. Again, the value we would measure is difficult to predict as it will depend on the concentration of each variant in the sample. With x_1' along one of the directions $\langle 10\text{-}1\rangle_C$ in the $(111)_C$ plane one domain type will contribute +8.0 pC/N and the other two will contribute −31.8 pC/N. Here, surprisingly, different domains will contribute transverse piezoelectric coefficients of different sign to the measured value. It is interesting to speculate on the possibility of having a zero net d_{31}^* at some partition of concentrations of the two domain variants.

C. Barium titanate ($BaTiO_3$)

The simplest domain-engineered structure for the $4mm$ tetragonal class, $2T$, is that formed by poling along the $[101]_C$ direction. The two resultant variants have polar axes (x_3) equally inclined to the poling direction. Starting with the monodomain defined in Fig. 1(c) and the values given in Table II (with $\phi=90°$ and $\theta=45°$), we calculate a value of $d_{33}^*=219.4$; this is more than twice the corresponding monodomain value of $d_{33}=90$ pC/N (see Table IV).

In this case $d_{31}^*(\phi=90°, \theta=45°, \psi)$ varies greatly between $X=-23.6$ pC/N (for x_1': $\pm[010]_C$) and $Y=-179.4$ pC/N (for x_1': $\pm[10\text{-}1]_C$); $\psi=0°$ here corresponds to x_1':$[010]_C$. The results are plotted in the $(101)_C$ plane for all choices of x_1' in Fig. 8(a). The most negative d_{31}^* value is found for x_1': $\pm[10\text{-}1]_C$, i.e., again parallel to the projection of the polar axis $[001]_C$ in the $(101)_C$ plane.

Since in the $2T$ structure, as in the $2R$ structure, the two variants are related to each other by a rotation of $\Delta\psi=180°$, they will both yield the same value of d_{31}^*. Therefore, we can engineer the crystal to have a predictable d_{31}^* value of either −23.6, −75.5, −127.5, or −179.4 pC/N.

The structure $3T$ is more interesting, and has already been the subject of investigation.[8,18] d_{33}^* (at $\phi=-45°$, $\theta=-54.74°$) for the $[111]_C$ direction was calculated as 221.5 pC/N, comparing favorably with the experimental value of 203 pC/N.[8] It is slightly higher that the value found for the $2T$ structure. d_{31}^* as a function of ψ (for $\phi=-45°$ and $\theta=-54.74°$) varies between $X=-19.3$ pC/N (at x_1': $\pm[1\text{-}10]_C$) and $Y=-188.9$ pC/N (at x_1': $\pm[11\text{-}2]_C$); $\psi=0°$ corresponds to x_1':$[1\text{-}10]_C$. The results are shown graphically in Fig. 8(b). For a variant with $\mathbf{P}_S(x_3)$:$[001]_C$, the most negative d_{31}^* is found by cutting the crystal with x_1': $\pm[11\text{-}2]_C$.

Since in the $3T$ structure all three variants are rotated by $\Delta\psi=120°$ relative to each other, the set of three d_{31}^* contributions from the three domain types will be separated by 120° in Fig. 8(b). Thus, if we choose x_1' parallel to one of the directions $\langle 11\text{-}2\rangle_C$ in the $(111)_C$ plane, two variants will contribute $d_{31}^*=-61.7$ pC/N and the other one will contribute −188.9 pC/N. However, if we choose x_1' parallel to one of the directions $\langle 10\text{-}1\rangle_C$ two variants will contribute $d_{31}^*=-146.5$ pC/N and the third will contribute −19.3 pC/N. Again, the actual d_{31}^* measured will depend on which domains are present and in what quantity.

The fact that different variants in a domain-engineered structure can contribute different values of d_{31}^* to that measured is perhaps not expected, especially since no similar effect is possible for d_{33}^*. In fact, excepting the $[101]_C$-poled structures, $2R$ and $2T$, the effect is general. Only in the $[001]_C$-poled $4O$ and $4R$ structures can the potential problem be avoided by careful choice of x_1'. Therefore, $[111]_C$-poled structures like those of $4mm$ barium titanate ($3T$) and $mm2$ potassium niobate ($3O$) are best avoided when domain engineering crystals are for use in the transverse mode, unless the presence of the undesired variants can be minimized.

When we do have a structure with differing d_{31}^* contributions from each domain variant, it is not trivial to predict the measured value. For calculations of d_{33}^* in domain-engineered structures, most researchers have settled on taking a volume average, often assuming that all domain families in the structure will be present in equal measure. Yet, the real domain structure in domain-engineered crystals, or the relative proportions of each domain, is actually difficult to predict. For example, in $4R$ PMN–xPT and PZN–xPT a prevalence of just two of the four domain types is possible leading to a macroscopically orthorhombic, not tetragonal, crystal.[6] Although in this case the measured value of d_{33}^* should be the same, d_{31}^* might not (depending on the choice of x_1'). It is even possible that in structures such as $3T$ barium titanate, where the d_{31}^* contribution from one variant can be much larger than from the other two, this imbalance might mean that one type of domain is formed preferentially upon poling if strain compatibility is important. This is a nontrivial problem, which is worthy of future analysis.

The physical reason behind the differing d_{31}^* contributions from different variants can be explained as follows: Looking at a projection of a tetragonal domain in the $(111)_C$ plane (Fig. 9), we see that there are always two equivalent directions for the transverse direction x_1' in our d_{31}^* sample, relative to the polar direction (x_3), and one which is unique. For simplicity, this is shown on the diagram for x_1' along $\langle 11\text{-}2\rangle_C$ directions only. It follows, therefore, that for a fixed x_1' direction in a $3T$-poled crystal, we may get one unique and two equal contributions to d_{31}^*. The question remains,

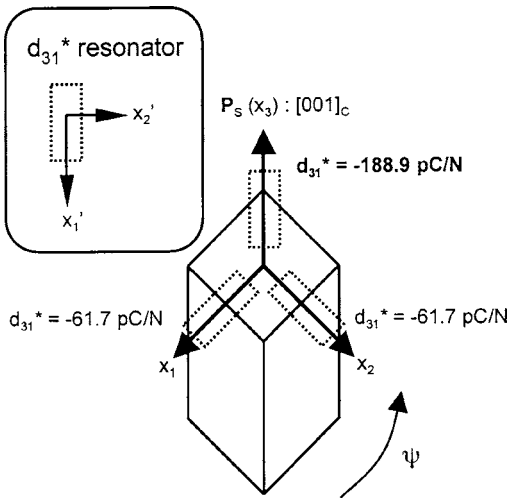

FIG. 9. Schematic illustrating the relationship between the tetragonal monodomain and the possible values of d_{31}^*, in the $3T$-engineered structure, for different choices of measurement direction x_3'. The polar axis $\mathbf{P}_S$ of the domain is shown projected in the $(111)_C$ poling plane. The most negative value of d_{31}^* is found when x_1' is parallel to this projection.

why do we get the most negative d_{31}^* contribution when x_1' is parallel to the projection of the domain's polar axis in the $(001)_C$ poling plane? When we apply an electric field along the poling direction x_3', the polar axis x_3 will rotate towards it (and away from the plane of Fig. 9), causing the projection of the domain to shrink along its length. The largest contraction, and therefore the most negative d_{31}^*, will be seen where x_1' is parallel to that direction. This "polarization rotation" effect[26] is strongest in materials where the piezoelectric shear coefficient d_{15} is large.[14]

D. Lead titanate ($PbTiO_3$)

Finally, calculations were made for the $3T$ structure formed by poling lead titanate along the $[111]_C$ direction. d_{33}^* (at $\phi=-45°$, $\theta=-54.74°$) was calculated as 27.9 pC/N (Table IV), lower this time than the monodomain value of 79.1 pC/N. Lead titanate is tetragonal over all temperatures below the Curie temperature: there are no ferroelectric-ferroelectric phase transitions.[23] Because of the absence of a proximal phase transition, the shear coefficient d_{15} is small (compare $PbTiO_3$ and $BaTiO_3$ in Table II) and the anisotropy of the piezoelectric tensor d_{ijk} is much weaker.[14] In fact, the maximum value of d_{33}^* for $PbTiO_3$ is that measured along its polar axis (i.e., that due to the collinear piezoelectric effect).

The most interesting effect occurs for the transverse coefficient. $d_{31}^*(\phi=-45°, \theta=-54.74°, \psi)$ is given in Table V and varies between $X=-13.3$ pC/N (at $x_1':\pm[1\text{-}10]_C$) and $Y=+4.4$ pC/N (at $x_1':\pm[11\text{-}2]_C$); $\psi=0°$ corresponds to $x_1':[1\text{-}10]_C$. In this case the general form of the equation is switched relative to $3T$ $BaTiO_3$. The values are plotted figuratively in the $(111)_C$ poling plane in Fig. 10. It is noticeable that for certain choices of x_1' (along $\pm[10\text{-}1]_C$ or $\pm[01\text{-}1]_C$) d_{31}^* is close to zero. Most importantly, in contrast to all of the other domain-engineered structures investigated, the direction that coincides with the projection of the polar axis is that of most *positive* d_{31}^*, not most negative. This can again be understood with reference to Fig. 9. For $PbTiO_3$, in contrast

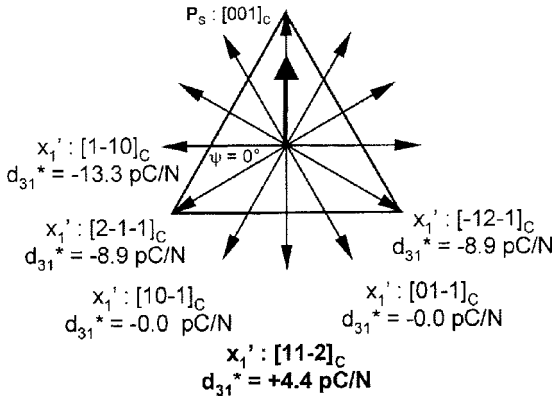

FIG. 10. The $(111)_C$ poling plane of a $3T$ sample of $PbTiO_3$ (with $x_3':[111]_C$). The values of d_{31}^* calculated for various choices of measurement direction x_1' are shown for a domain with spontaneous polarization $\mathbf{P}_S$ (or x_3):$[001]_C$ ($\mathbf{P}_S$ is also shown projected onto the plane as a thick arrow). The most *positive* value is shown in bold and lies at $x_1':\pm[11\text{-}2]_C$.

to the other three, the collinear piezoelectric effect is more important than polarization rotation.[26] That is, as explained above, d_{33}^* is highest along the polar axis due to a weak contribution from d_{15}. Therefore, upon application of an electric field along $[111]_C$, the projected tetragonal domain will expand along its projected length more than it will contract due to polarization rotation. d_{31}^* is thus positive for $PbTiO_3$ when x_1' is parallel to its projected polar axis. Lead titanate will form domain-engineered structures with properties unlike the other three materials at room temperature.

IV. CONCLUSIONS

Calculations have been made of the longitudinal and transverse piezoelectric coefficients, d_{33}^* and d_{31}^*, in the six possible domain-engineered structures for rhombohedral PMN–33PT, orthorhombic $KNbO_3$, and tetragonal $BaTiO_3$ at room temperature. The tetragonal ($3T$) domain-engineered structure formed in $BaTiO_3$ by poling along $[111]_C$ has been compared to that of $PbTiO_3$. The main conclusions of this paper are as follows:

Firstly, for all domain-engineered structures, d_{31}^* is strongly dependent on the choice of the measurement direction x_1' in the plane of the crystal perpendicular to the poling direction x_3', whereas d_{33}^* is not. Care is therefore required when cutting a domain-engineered crystal for use in the transverse mode.

In general, different variants in a domain-engineered structure will contribute *different* values of d_{31}^* to that measured. This is never the case for d_{33}^* certainly, at least, for the $3m$, $mm2$, and $4mm$ crystal classes. It follows, that the actual value of d_{31}^* measured will be a nontrivial function of the relative proportions of each domain variant. The value of d_{31}^* is thus difficult to predict unless the domain structure of the material can be controlled. This problem is avoided completely in $\langle 101\rangle_C$-poled domain-engineered structures ($2R$ and $2T$) and can be avoided in the $\langle 001\rangle_C$-poled $4R$ and $4O$ structures by careful choice of x_1'. In fact, recent work suggests that in some cases (e.g., $3T$),[27] it may be possible to avoid undesired variants entirely via careful control of the

poling conditions.[1]

A very high value of d_{31}^* (−1630 pC/N) is predicted for the 2*R* domain structure formed by PMN–33PT, via a careful choice of x_1'. Similarly high values have recently been measured experimentally for 2*R* PMN–30PT.[20]

Finally, key differences have been highlighted between the tetragonal phases in $BaTiO_3$ and $PbTiO_3$. Room-temperature barium titanate exhibits its largest longitudinal piezoelectric coefficient d_{33}^* away from its polar axis as do PMN–33PT and $KNbO_3$. In these materials, polarization rotation is significant upon application of an off-polar axis field, behavior related to their large shear coefficients (d_{15}). In contrast, monodomain $PbTiO_3$ has a low d_{15} and exhibits its maximum d_{33}^* along the polar axis. That is, it demonstrates a collinear piezoelectric effect much stronger than the effect of rotation of its polarization, a fact related to the lack of ferroelectric phase transitions in $PbTiO_3$. This property of lead titanate leads to low d_{33}^* coefficients in the 3*T* domain-engineered structure and, more surprisingly, positive d_{31}^* values that do not occur in the equivalent $BaTiO_3$ structure.

The methodology used can be followed to make similar calculations for domain-engineered structures based on other materials; this might be helpful in designing future crystals for use in the transverse piezoelectric mode.

ACKNOWLEDGMENT

The authors acknowledge financial support from the Swiss National Science Foundation.

[1]Erhart and Cao[28] find that the $[111]_C$-poled 3*O* and 3*T* structures do not have two-dimensional translational symmetry and hence are not permissible. The experimental results in Ref. 27 suggest that for 3*T* barium titanate only two of the three domain variants form upon poling; interestingly, these are the two variants that contribute the same value of d_{31}^* [see Fig. 8(b)].

[1]S.-E. E. Park and T. R. Shrout, J. Appl. Phys. **82**, 1804 (1997).
[2]A. J. Bell, J. Appl. Phys. **89**, 3907 (2001).
[3]T. Liu and C. S. Lynch, Acta Mater. **51**, 407 (2003).
[4]D. Liu and J. Li, Appl. Phys. Lett. **84**, 3930 (2004).
[5]R. Zhang, B. Jiang, and W. Cao, J. Appl. Phys. **90**, 3471 (2001).
[6]J. Yin and W. Cao, J. Appl. Phys. **92**, 444 (2002).
[7]H. Dammak, A.-E. Renault, P. Gaucher, M. P. Thi, and G. Calvarin, Jpn. J. Appl. Phys., Part 1 **42**, 6477 (2003).
[8]S. Wada *et al.*, Jpn. J. Appl. Phys., Part 1 **38**, 5505 (1999).
[9]S. Wada, K. Muraoka, H. Kakemoto, T. Tsurumi, and H. Kumagai, Jpn. J. Appl. Phys., Part 1 **43**, 6692 (2004).
[10]K. Nakamura, T. Tokiwa, and Y. Kawamura, J. Appl. Phys. **91**, 9272 (2002).
[11]R. Zhang, B. Jiang, and W. Cao, Appl. Phys. Lett. **82**, 787 (2003).
[12]R. Zhang and W. Cao, Appl. Phys. Lett. **85**, 6380 (2004).
[13]M. Zgonik *et al.*, Phys. Rev. B **50**, 5941 (1994).
[14]M. Budimir, D. Damjanovic, and N. Setter, J. Appl. Phys. **94**, 6753 (2003).
[15]R. Zhang, B. Jiang, and W. Cao, Appl. Phys. Lett. **82**, 3737 (2003).
[16]D. Damjanovic, M. Budimir, M. Davis, and N. Setter, Appl. Phys. Lett. **83**, 527 (2003).
[17]D. Damjanovic, M. Budimir, M. Davis, and N. Setter, Appl. Phys. Lett. **83**, 2490 (2003).
[18]S. Wada, H. Kakemoto, and T. Tsurumi, Mater. Trans., JIM **45**, 178 (2004).
[19]V. Y. Topolov, J. Phys.: Condens. Matter **16**, 2115 (2004).
[20]J. Peng, H.-S. Luo, D. Lin, H.-Q. Xu, T.-H. He, and W.-Q. Jin, Appl. Phys. Lett. **85**, 6221 (2004).
[21]J. F. Nye, *Physical Properties of Crystals*, 2nd ed. (Clarendon, Oxford, 1985).
[22]M. Zgonik, R. Schlesser, I. Biaggio, E. Voit, J. Tscherry, and P. Gunter, J. Appl. Phys. **74**, 1287 (1993).
[23]Z. Li, M. Grimsditch, X. Xu, and S.-K. Chan, Ferroelectrics **141**, 313 (1993).
[24]M. J. Haun, E. Furman, S. J. Jang, H. A. McKinstry, and L. E. Cross, J. Appl. Phys. **62**, 3331 (1987).
[25]H. Goldstein, *Classical Mechanics* (Addison-Wesley, Reading, MA, 1978).
[26]H. Fu and R. E. Cohen, Nature (London) **403**, 281 (2000).
[27]S. Wada, K. Yako, H. Kakemoto, T. Tsurumi, D. Damjanovic, A. J. Bell, and L. E. Cross (unpublished).
[28]J. Erhart and W. Cao, J. Appl. Phys. **94**, 3436 (2003)